

IMPACT OF WINDOW SHADING ON THE THERMAL PERFORMANCE OF RESIDENTIAL BUILDINGS OF DIFFERENT FORMS IN JORDAN

Esraa Sh. Abbaas^{*1}, Mazran Ismail^{**1}, Ala'eddin A. Saif², Muhamad Azhar Ghazali¹

¹School of Housing, Building and Planning, Universiti Sains Malaysia
Penang, Malaysia

²College of Science, University of Jeddah
Jeddah, Saudi Arabia

Corresponding author's e-mail: *esraabbas91@gmail.com, **mazran@usm.my

Abstract

Introduction: Window shading is considered one of the most effective passive design approaches that improves indoor thermal performance, minimizing the usage of HVAC and reducing energy consumption. **Purpose of the study:** We aimed to investigate the impact of external window shading on thermal performance of three existing residential buildings having different forms (rectangular, L-shaped, and U-shaped) in hot-dry climate in Amman, Jordan. **Methods:** Three types of shading, namely: vertical, horizontal, and combined, of different lengths (0.75 m, 1.00 m, and 1.25 m) were introduced to the existing buildings. The effect of those types of shading was studied using the OpenStudio SketchUp 2020 plugin and EnergyPlus simulation program. **Results:** It was established that vertical shading slightly improves the indoor air temperature in all building forms, while horizontal shading and combined shading improve the thermal performance of buildings to a more significant extent. Combined shading of 1.25 m in length shows the optimum behavior in all buildings since it reduces the indoor air temperature in the range of 2.6–3.3°C. Besides, it improves thermal sensation, which seem to be closer to the comfort zone, by reducing the predicted mean vote (PMV) and predicted percentage of dissatisfied (PPD) values as compared with the baseline situation without shading. In addition, the rectangular building demonstrated the best response for shading by showing the largest reduction in the indoor air temperature.

Keywords: EnergyPlus, shading, thermal comfort, PMV, hot-dry climate, residential building.

Introduction

Windows are responsible for a large share of heat gain during summer and heat loss during winter in buildings. A number of solutions have been proposed to minimize energy exchange through windows such as the use double glazing and window shading or decrease in the window-wall ratio (Bataineh and Alrabee, 2018). Shading devices significantly improve the thermal performance of buildings by reducing heat gain since they block direct sunlight in summer and reduce heat losses in winter, thus minimizing the cooling and heating loads and saving energy (Mushtaha et al., 2021). Generally, shading of openings includes exterior and interior window shading. Exterior window shading is more effective in minimizing the heat gain of direct sunlight than interior window shading. However, interior window shading is more advantageous since it offers more user-friendly control (Ohene et al., 2022). There are other types of shading ensured by architectural elements such as Iwan, which is more popular in the Middle Eastern and North African architecture (Eskandari et al., 2018). Shading effect can also be

achieved thanks to tall trees improving the thermal performance of the buildings nearby (both residential and commercial) in hot climate (Minangi and Alibaba, 2018). Window shading is considered the most effective since it can be adjusted to minimize solar radiation received by the building (Feng et al., 2021). Besides, the availability of numerous kinds of window shading on the market in a wide range of prices makes them the preferable choice of occupants (especially in residential buildings) who install them even at the late stage of construction to achieve the optimal thermal comfort.

Some researchers investigated the impact of using different types of shading on the thermal performance and energy consumption of various buildings in Jordan. For instance, Freewan (2014) analyzed the effect of using three window shading devices (egg crate, vertical fins, and diagonal fins) on the air temperature of the south-west facade of an office building in Irbid, Jordan. He found that those shading devices can improve the indoor air temperature returning it to the acceptable range compared to the office without shading devices.

Moreover, egg crate and diagonal fins showed better performance in terms of improving air temperature compared to vertical fins. Ali and Hashlamun (2019) studied the effect of adding 100 cm horizontal overhang on the southern facade of a school in Amman on energy saving in terms of both cooling and heating. They established that the proposed shading system can save 20.3% of annual cooling energy but shows minimum effect regarding energy saved on heating, which amounts to 9.8%. Abu Qadourah et al. (2022) examined the impact of such shading devices as horizontal shading on the southern facade and horizontal fins on the eastern facade, having different lengths, in a multi-family apartment building in Amman, Jordan. They found that both types of shading can decrease the cooling energy demand and increase the heating and lighting energy demands. In addition, an increase in the size of the shading devices enhances their effect.

We have noticed that only a limited number of works focused on investigating the effect of window shading on thermal performance and thermal comfort in Jordan, while most of them dealt with window shading devices as passive design strategies to improve energy performance (Abu Qadourah et al., 2022; Bataineh and Alrabee, 2018; Bataineh and

Al Rabee, 2021). Therefore, this study addresses the influence of different types of exterior shading, particularly: vertical fins, horizontal overhang, and the combined structure of vertical and horizontal shading, on the thermal performance and thermal comfort of existing residential buildings of different forms (rectangular, L-shaped, and U-shaped) in Amman, the capital of Jordan. To study the impact of shading on the thermal performance of these buildings, we analyzed the indoor air temperature and evaluated its influence on the thermal comfort of the buildings using the predicted mean vote (PMV) and predicted percentage of dissatisfied (PPD) indicators.

Methods

Case studies

We considered three case studies representing different residential building forms, namely: rectangular, L-shaped, and U-shaped, located in the same district of Amman. Fig. 1 shows photos of the main facades of those buildings facing the west. All buildings have the same constructions and consist of three floors. Only three west-facing rooms (one on the middle floor of each building) were taken for this study. We investigated the impact of vertical fins, horizontal overhang, and the combined structure of



Fig. 1. Main facades of the buildings of different forms: (a) rectangular, (b) L-shaped, and (c) U-shaped

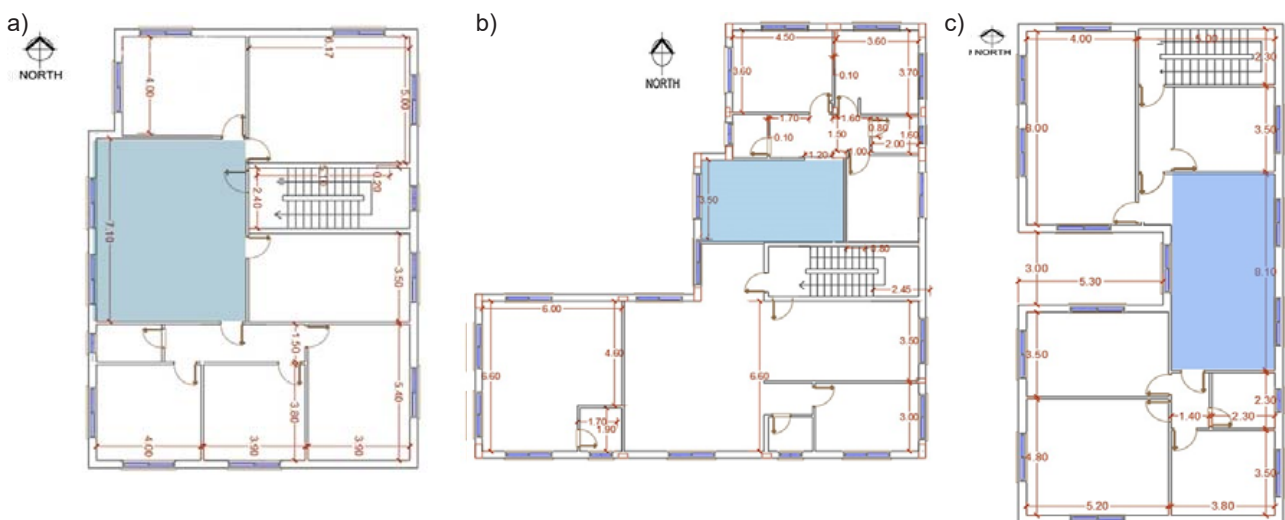


Fig. 2. 2D plans with the rooms in the buildings of different forms: (a) rectangular, (b) L-shaped, and (c) U-shaped

vertical and horizontal shading of different lengths on the thermal performance of these rooms. We also analyzed the thermal comfort of these rooms using the PMV and PPD indicators. Fig. 2 shows the middle floor plan of each of the three buildings where the west-facing rooms under consideration are highlighted with blue color. These rooms were selected since the west facade is facing solar radiation for longer time during the day (see the sun path chart in Fig. 3).

Amman, the capital of Jordan, lies at latitude 31°57'23.76" North and longitude 35°56'44.52" East. About 90% of Jordan areas are semi-arid or arid since the climate is mainly of the Mediterranean type, hot in summer and cold in winter (Abdulla, 2020). We focused on the hot-dry summer season, which lasts for three months from June 21 to September 21, where July 21 July was picked as the design day. In summer, the air temperature at peak hours from 1:00 PM to 3:00 PM can be as high as 40°C (Albatayneh et al., 2021). Besides, summer in Amman is known to have long daytime hours, where on July 21 they lasted from 5:45 AM until 7:40 PM, which is about 14 hours (Table 1). This means that the buildings are exposed to sun radiation for long time during the daytime.

For further understanding of summertime and solar radiation in Amman, which is located both in the northern and eastern hemispheres, we need to analyze the sun path. The sun path is the seasonal and daily arc that Sun follows as the Earth goes around the Sun throughout the year. The sun path affects the length of the daytime and the amount of solar radiation received by the buildings at certain time during the day or season. Besides, the sun altitude and azimuth play an important role in the amount of shading cast on a building by the surrounding buildings and trees (Nwankwo et al., 2021).

We downloaded the polar sun path chart for Amman (Fig. 3) using the sun path tool available on sunearthtools.com. Here, the orange line represents the sun path on July 21. The polar chart shows the Sun elevation, azimuth, clock line, and date line. Another type of chart for the Sun path is the Cartesian chart (not shown), where the Sun position is plotted hourly by the solar elevation angle

Table 1. Amman, Jordan — sunrise, sunset, dawn and dusk times (GIASMA, 2022)

Date	sunrise	sunset	dawn	dusk
July 21, 2022	5:45	19:40	5:18	20:07

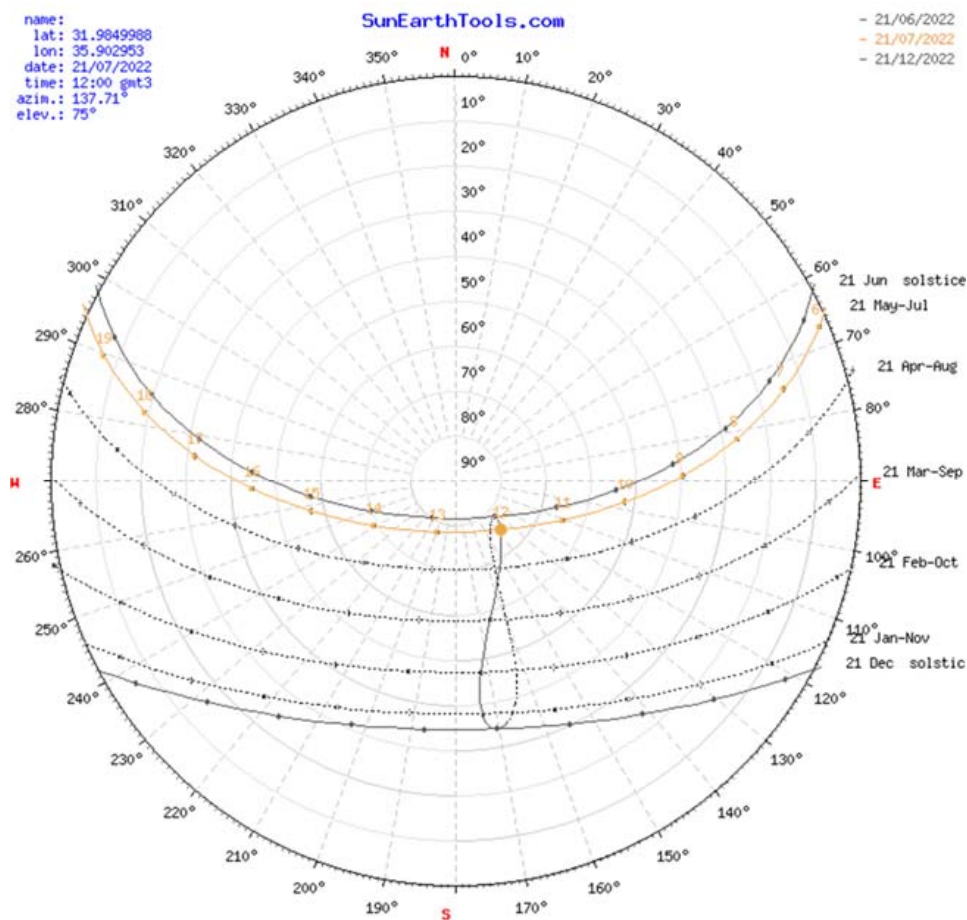


Fig.3. Polar sun path chart for July 21 in Amman, Jordan

as a function of the solar azimuth angle. According to the polar chart, at midday time (12:00 PM), the Sun was located at an azimuth angle of 137.71° and elevation angle of 75° . The estimated track angle for the Sun from 12:00 PM till sunset was 157.1° , while the track angle from sunrise till 12:00 PM was 72.66° . This means that the west facades of the buildings would receive higher solar radiation as compared with the east facades. For further understanding of the Sun position effect during daytime and the times when the building facades are exposed to sun or shaded, the Sun path at 8:00 AM, 12:00 PM, and 4:00 PM was plotted for the buildings under consideration (Figs. 4–6). It should be noted that the azimuth and elevation angles at 8:00 AM were 81.46° and 26.61° , respectively,

while at 4:00 PM they were 267.78° and 44.67° , respectively. Based on Figs. 4–6, it can be seen that since the selected rooms face the west, they would be shaded in the morning (except for the room in the U-shaped building, which has two windows facing the east, exposed to sun in the morning) and receive the afternoon sun.

Simulation

We performed a simulation study to investigate the effect of shading devices on the thermal performance and thermal comfort of the residential buildings of different forms located in Amman. To do that, we started with the measurement of environmental parameters at the sites, i.e., air temperature, air velocity, mean radiant temperature, and relative humidity regarding the baseline situation with the windows closed and

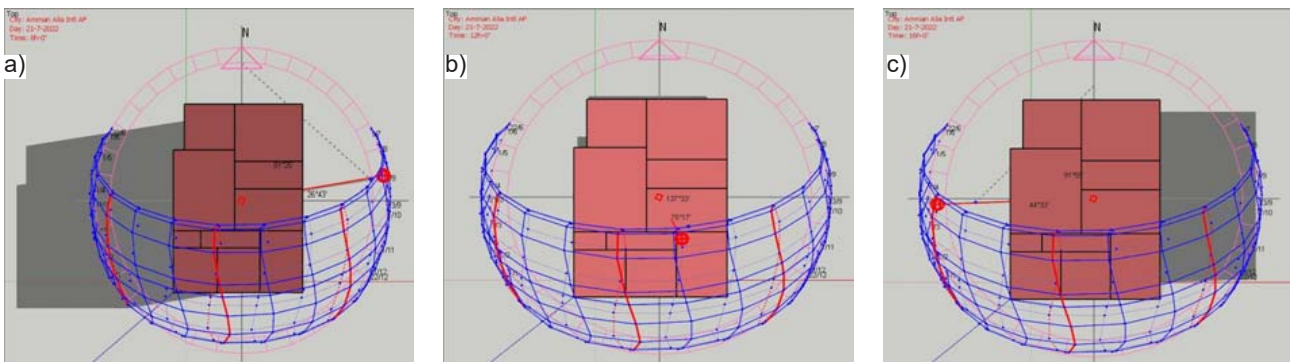


Fig. 4. Sun path diagram for the rectangular building on July 21 at (a) 8:00 AM, (b) 12:00 PM, and (c) 4:00 PM

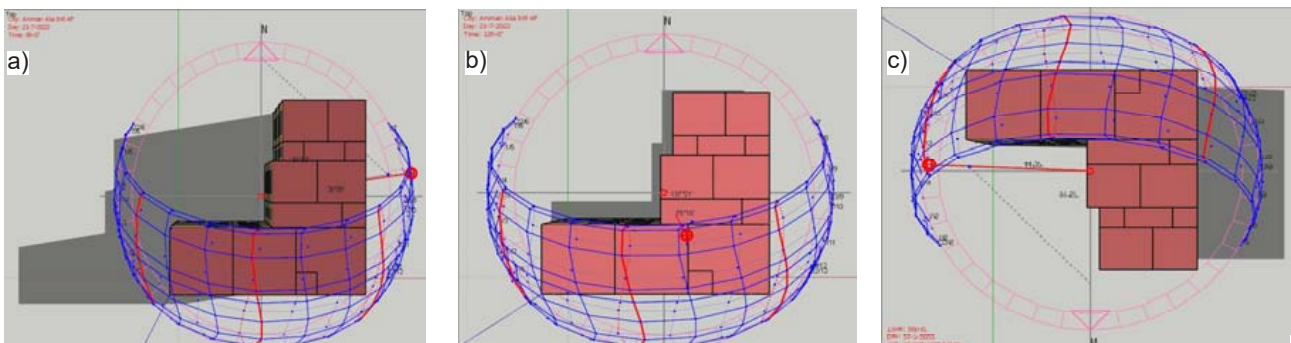


Fig. 5. Sun path diagram for the L-shaped building on July 21 at (a) 8:00 AM, (b) 12:00 PM, and (c) 4:00 PM

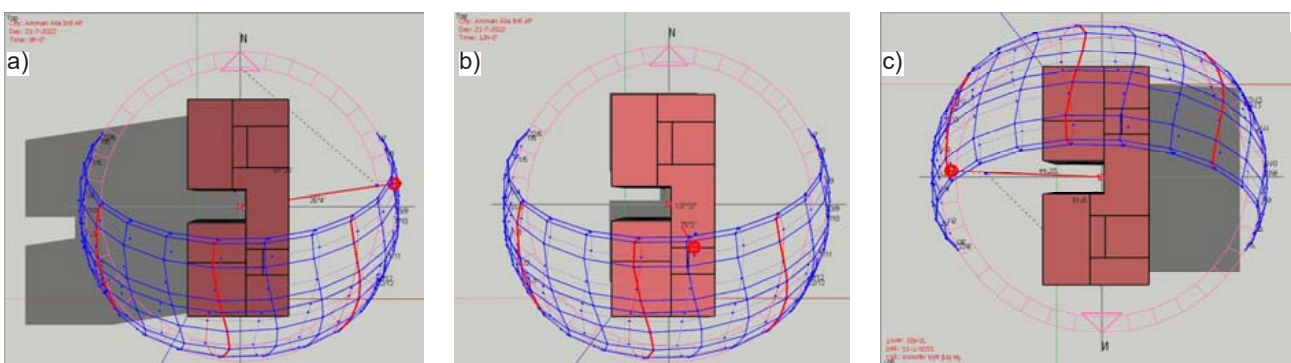


Fig. 6. Sun path diagram for the U-shaped building on July 21 at (a) 8:00 AM, (b) 12:00 PM and (c) 4:00 PM

without shading. These measurements were used to validate the simulation results, and they were found to be very close to each other.

At the early stage of simulation, we drew two-dimensional plans of the buildings of different forms using AutoCAD, and then built three-dimensional models for all the three buildings using the OpenStudio SketchUp 2020 plugin. In the existing buildings, we determined the construction system for the roof, walls, and ground. We also determined characteristics of each building space (where the space type was selected as residential), and set the number of floors to be equal to three. Then we uploaded the climate file for Amman in the EPW format to the OpenStudio platform. July 21 was imported in the DDY format as the summer design day. Besides, we defined the infiltration schedules and internal loads such as people, electric equipment, and light for the spaces. Finally, models were simulated in baseline situations without shading using the EnergyPlus simulation program.

The impact of shading on the thermal performance of the buildings (rooms under consideration) was studied by introducing different types of shading, particularly: vertical fins, horizontal overhang, and combined shading structure. These shading devices had different lengths of 0.75 m, 1.00 m, and 1.25 m. For more accuracy, the output environmental parameters were set to be simulated every 15 minutes, and then four readings per hour were averaged. The thermal performance of the buildings was analyzed based on the indoor air temperature. The air temperature in the rooms was measured with the presence of shading devices while the windows were closed, both individually and compared to the

baseline case without shading. Finally, the output environmental parameters were used to evaluate the thermal comfort of the buildings by studying the PMV and PPD indicators for the baseline situation and for the optimum type of shading at its optimum length. Figs. 7–9 show different types of shading devices for three building forms: vertical shading (fins), horizontal shading (overhang), and combined shading, respectively. These types of shading were investigated at three different shading device lengths of 0.75 m, 1.00 m, and 1.25 m.

Results and discussion

Air temperature depending on the type of shading device in the buildings of different forms

Fig. 10 shows the effect of the vertical, horizontal and combined shading devices having different lengths on the thermal performance of the rectangular building. It can be seen that all shading devices have a notable impact on reducing the air temperature in the room as compared with the baseline case without shading. Furthermore, one can notice that as the length of the shading device increases, the indoor air temperature slightly decreases. For instance, in Fig. 10a, the air temperature slightly decreases with the presence of vertical shading fins in the range of 0.4–0.6°C regardless of length as compared with the baseline situation. While in the presence of horizontal overhang shading, the air temperature shows better results since it decreases by 2.1°C, 2.5°C, and 2.8°C at an overhang length of 0.75 m, 1.00 m, and 1.25 m, respectively, as compared with the case without shading at 4:00 PM (Fig. 10b). In case of the combined shading structure, the air temperature shows the largest difference as compared with the case without shading: at a length

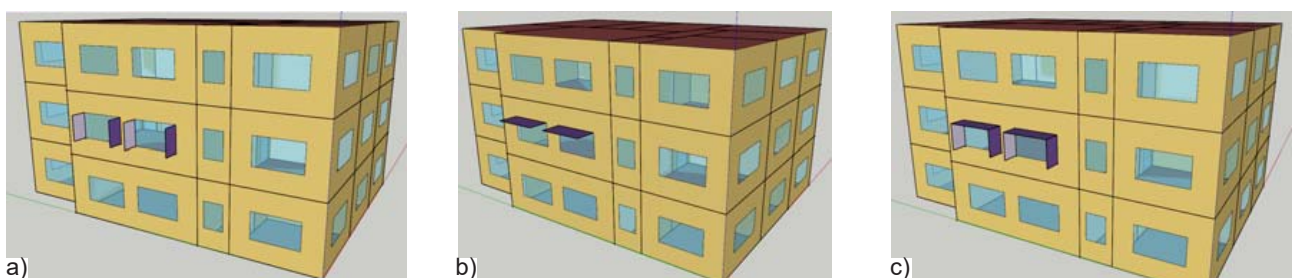


Fig. 7. Shading devices: (a) vertical shading (fins), (b) horizontal shading (overhang), and (c) combined shading for the rectangular building

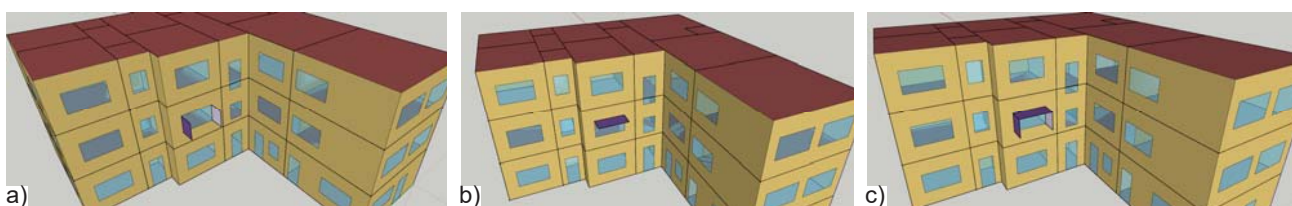


Fig. 8. Shading devices: (a) vertical shading (fins), (b) horizontal shading (overhang), and (c) combined shading for the L-shaped building

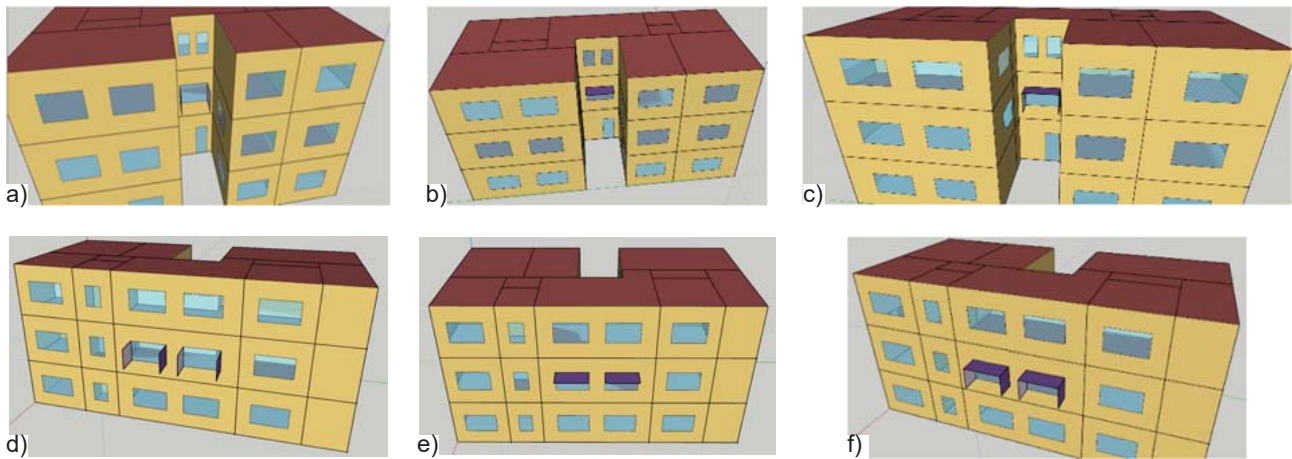


Fig. 9. Shading devices: (a) vertical shading (fins) of a west side window, (b) horizontal shading (overhang) of a west side window, (c) combined shading of a west side window (d) vertical shading (fins) of east side windows, (e) horizontal shading (overhang) of east side windows, and (f) combined shading of east side windows for the U-shaped building

of the shading device of 0.75 m, 1.00 m, and 1.25 m, the air temperature decreases by 2.4°C, 2.9°C, and 3.3°C at 4:00 PM, respectively (Fig. 10c).

A similar trend is observed for the air temperature in the presence of different shading devices as compared with the case without shading for the L-shaped building (Fig. 11). Fig.11a shows almost negligible air temperature reduction in the presence of vertical fins, where it reaches its maximum of 0.3°C at 1.25 m in length. On the other hand, in the

presence of horizontal overhang, the air temperature is characterized by a significant reduction of 1.8°C, 2.2°C, and 2.5°C at a length of 0.75 m, 1.00 m, and 1.25 m, respectively, as compared with the case without shading (Fig. 11b). The combined shading device shows the optimum behavior with regard to the air temperature by reducing the temperature by up to 1.9°C, 2.4°C, and 2.7°C at 4:00 PM at a length of 0.75 m, 1.00 m, and 1.25 m, respectively (Fig. 11c).

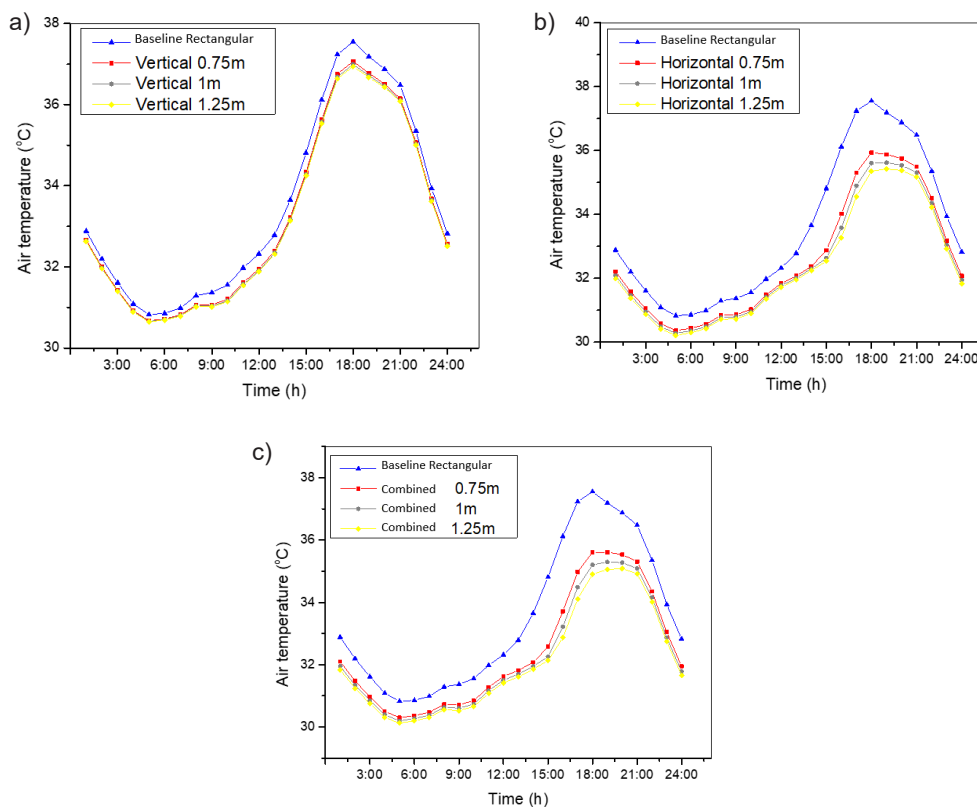


Fig. 10. Comparison of the air temperature in the rectangular building for different shading devices having different lengths: (a) vertical fins, (b) horizontal overhang, and (c) combined shading device

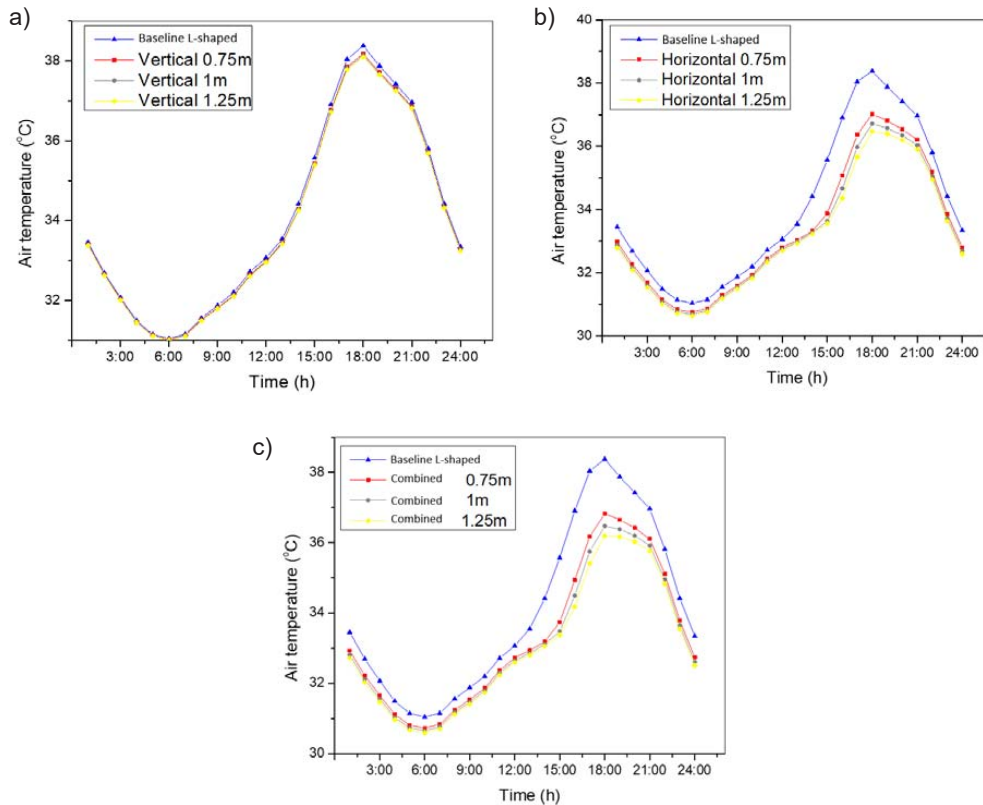


Fig. 11. Comparison of the air temperature in the L-shaped building for different shading devices having different lengths: (a) vertical fins, (b) horizontal overhang, and (c) combined shading device

A similar trend is observed for the indoor temperature reduction in the presence of shading devices in the U-shaped building as compared with the rectangular and L-shaped buildings (Fig. 12). As compared with the case without shading, vertical fins ensure the maximum air temperature difference of 0.35°C at a length of 1.25 m (Fig. 12a). While in case of horizontal overhang, larger air temperature differences are noticed (Fig. 12b), where at 10:00 AM, the temperature difference of 2.2°C , 2.6°C , and 2.9°C is recorded for 0.75 m, 1.00 m, and 1.25 m of length, respectively. At 4:00 PM, the temperature difference of 1.7°C , 2.0°C , and 2.3°C is recorded at the same length values, respectively. Fig. 12c shows the performance of combined shading at different lengths, where the air temperature reduction is also noteworthy: the temperature difference reaches 2.4°C , 2.5°C , and 3.2°C at 10:00 AM and 1.9°C , 2.3°C , and 2.6°C at 4:00 PM at a length of 0.75 m, 1.00 m, and 1.25 m, respectively. These differences in the indoor temperature when using horizontal and combined shading at 10:00 AM in the U-shaped building are attributed to the existence of the east windows in addition to the west window. Moreover, the lower temperature reduction at 4:00 PM as compared with that obtained at 10:00 AM is due to self-shading as a result of the U-shape for the west window, which is predominant during daytime (Fig. 6). Thus, extra shading would have less effectiveness

as compared with the east windows exposed directly to the sun during morning hours where shading devices make more obvious difference.

Based on the discussion for Figs. 10–12, it can be concluded that for all proposed types of shading, the optimum length is equal to 1.25 m. This means that the longer the shading device, the better shading effect is obtained, which results in lower temperature values. To determine the optimum shading device to be used for each building form, the air temperature during the day was plotted for different types of shading with a length of 1.25 m for each building form (Fig. 13). The results show that the vertical fins demonstrates the lowest temperature difference of $0.3\text{--}0.6^{\circ}\text{C}$ as compared with the baseline case without shading for all building forms. This indicates that the use of vertical fins on the west facade is not practical. The horizontal overhang shows better performance as it reduces the indoor air temperature by $2.3\text{--}2.9^{\circ}\text{C}$ for all building forms. Besides, it is considered practical for the exterior facade and ensures better view as compared with the vertical fins. The combined shading device shows the optimum results for all building forms in terms of reducing the air temperature since the lowest values of $2.6\text{--}3.3^{\circ}\text{C}$ were recorded. Interestingly, the maximum reduction in the air temperature of 3.3°C was recorded for the rectangular building with combined shading.

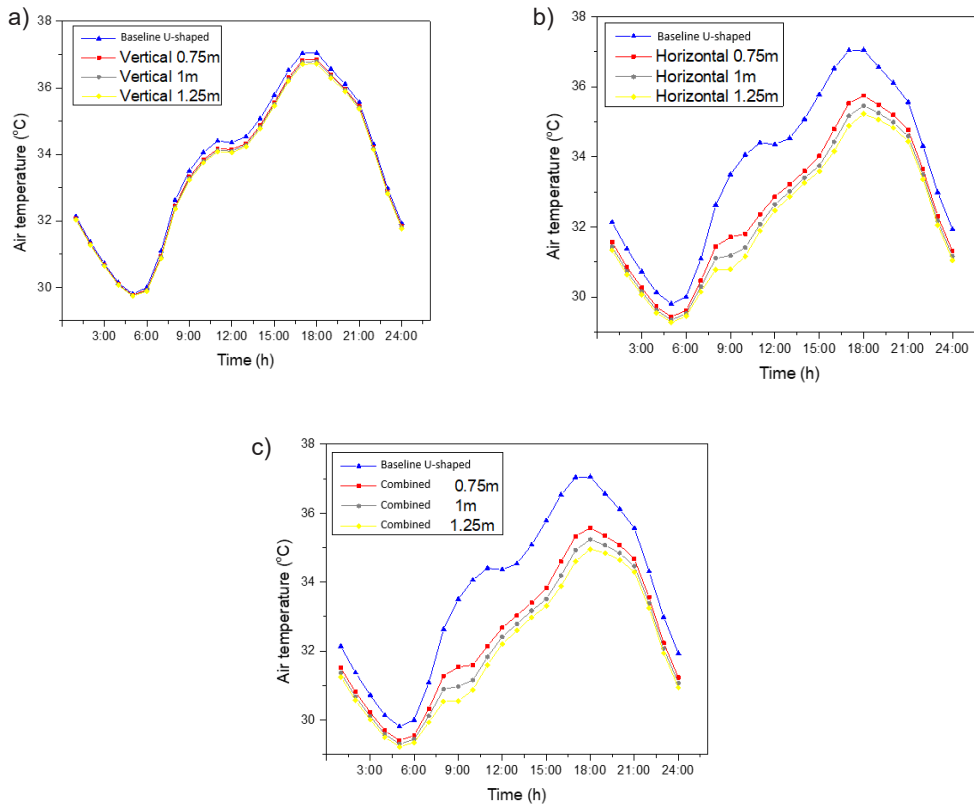


Fig. 12. Comparison of the air temperature in the U-shaped building for different shading devices at various lengths: (a) vertical fins, (b) horizontal overhang, and (c) combined shading device

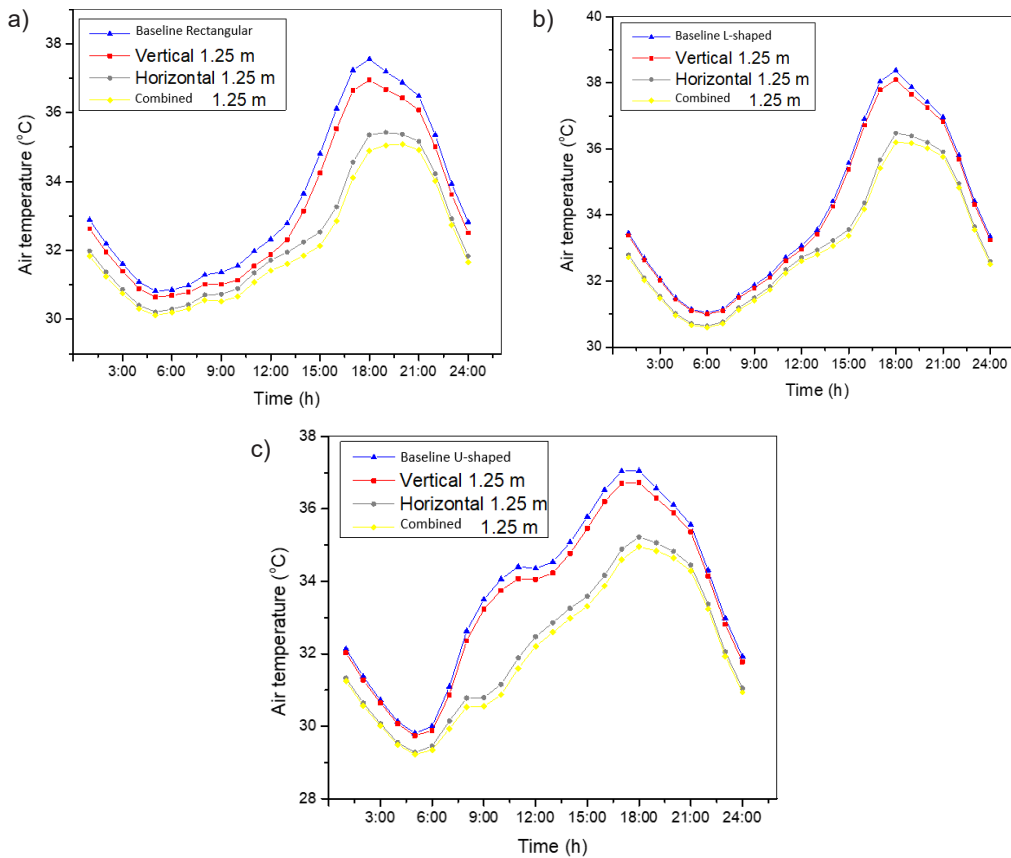


Fig. 13. Comparison of the air temperature for different shading devices with the optimum length (1.25m) for different building forms: (a) rectangular, (b) L-shaped, and (c) U-shaped

Table 2. Seven-point thermal sensation scale according to Fanger's model (Fanger, 1970)

Scale	Sensation
3	Hot
2	Warm
1	Slightly warm
0	Neutral
-1	Slightly cool
-2	Cool
-3	Cold

PMV and PPD of different shading devices for different building forms

To gain a better understanding of the impact of shading devices on the thermal performance of the buildings under consideration, the optimal shading device (combined shading) was compared with the baseline case without shading using the predicted mean vote (PMV) and predicted percentage of dissatisfied (PPD) indicators. The PMV and PPD indicators are usually determined with the use of Fanger's model, which was originally developed by collecting data from a large number of surveys on people subjected to different conditions within a climate zone (Emir, 2016). The PMV indicator is the average comfort vote based on the seven-point

thermal sensation scale from cold -3 to hot +3 (Table 2), while the PPD indicator is used to evaluate the ability of occupants to withstand high and low air temperatures in terms of thermal comfort conditions (Duan et al., 2022; Fanger and Toftum, 2002; Hailu et al., 2021; Kumar and Sharma, 2022). For an indoor thermal zone to provide comfort sensation, the acceptable range of PMV should be in the range from -1 to +1 and PPD should be less than 26%.

According to Fanger's model, PMV can be calculated by the following equation (Duan et al., 2022; Rînjea et al., 2022):

$$PMV = \left(0.303e^{-0.036M} + 0.028 \right) \times \left\{ \begin{aligned} &M - W - 3.05 \times 10^{-3} \times \\ &\times [5733 - 6.99(M - W) - Pa] - \\ &- 0.42[(M - W) - 58.15] - \\ &- 1.72 \times 10^{-5} M(5867 - Pa) - \\ &- 0.0014M(34 - t_a) - 3.96 \times 10^{-8} f_{cl} \times \\ &\times [(t_{cl} + 273)^4 - (t_r + 273)^4 - f_{cl} h_c (t_{cl} - t_a)] \end{aligned} \right\}, \quad (1)$$

where M is the energy metabolic rate in W/m^2 , W is the effective mechanical power generated by the

Table 3. PMV, PPD, and thermal sensation for the west room in the rectangular building in the baseline case and with optimum shading devices 1.25 m long

Time (h)	PMV Rectangular Baseline	PPD Rectangular Baseline (%)	Sensation Rectangular Baseline	PMV Rectangular Combined	PPD Rectangular Combined (%)	Sensation Rectangular Combined
1:00	2.64	95.9	Warm	2.36	90.1	Warm
2:00	2.45	92.4	Warm	2.2	84.9	Warm
3:00	2.27	87.4	Warm	2.03	78.4	Warm
4:00	2.12	82	Warm	1.91	72.58	Slightly warm
5:00	2.00	76.8	Warm	1.8	67.2	Slightly warm
6:00	1.95	74.7	Slightly warm	1.77	65.7	Slightly warm
7:00	1.96	75.3	Slightly warm	1.78	66.4	Slightly warm
8:00	2.03	78.3	Warm	1.84	69.3	Slightly warm
9:00	2.08	80.3	Warm	1.88	71.1	Slightly warm
10:00	2.12	82.2	Warm	1.92	73	Slightly warm
11:00	2.19	84.6	Warm	1.99	76.3	Slightly warm
12:00	2.26	87.1	Warm	2.07	79.9	Warm
13:00	2.36	90.1	Warm	2.1	81.3	Warm
14:00	2.60	95.2	Warm	2.16	83.5	Warm
15:00	2.92	98.6	Warm	2.23	86.2	Warm
16:00	3.28	99.7	Hot	2.4	91.1	Warm
17:00	3.54	99.96	Hot	2.68	96.4	Warm
18:00	3.58	99.97	Hot	2.86	98.3	Warm
19:00	3.48	99.95	Hot	2.9	98.6	Warm
20:00	3.38	99.90	Hot	2.89	98.5	Warm
21:00	3.28	99.8	Hot	2.86	98.3	Warm
22:00	3.11	99.4	Hot	2.74	97.1	Warm
23:00	2.87	98.3	Warm	2.56	94.6	Warm
0:00	2.65	96.1	Warm	2.35	89.8	Warm

Table 4. PMV, PPD, and thermal sensation for the west room in the L-shaped building in the baseline case and with optimum shading devices 1.25 m long

Time (h)	PMV L-shaped Baseline	PPD L-shaped Baseline (%)	Sensation L-shaped Baseline	PMV L-shaped Combined	PPD L-shaped Combined (%)	Sensation L-shaped Combined
1:00	2.75	97.27	Warm	2.6	95.29	Warm
2:00	2.54	94.32	Warm	2.42	91.56	Warm
3:00	2.34	89.67	Warm	2.24	86.45	Warm
4:00	2.18	84.3	Warm	2.1	81.17	Warm
5:00	2.03	78.42	Warm	1.97	75.61	Slightly warm
6:00	1.96	75.07	Slightly warm	1.91	72.66	Slightly warm
7:00	1.95	74.71	Slightly warm	1.9	72.32	Slightly warm
8:00	2.02	77.75	Warm	1.97	75.57	Slightly warm
9:00	2.09	80.79	Warm	2.03	78.5	Warm
10:00	2.16	83.52	Warm	2.1	81.33	Warm
11:00	2.24	86.29	Warm	2.18	84.32	Warm
12:00	2.31	88.68	Warm	2.26	87.06	Warm
13:00	2.41	91.4	Warm	2.28	87.91	Warm
14:00	2.64	95.83	Warm	2.33	89.26	Warm
15:00	3	98.99	Hot	2.41	91.46	Warm
16:00	3.37	99.87	Hot	2.59	95.12	Warm
17:00	3.66	99.98	Hot	2.89	98.45	Warm
18:00	3.73	99.99	Hot	3.09	99.44	Hot
19:00	3.63	99.98	Hot	3.15	99.6	Hot
20:00	3.51	99.96	Hot	3.14	99.57	Hot
21:00	3.4	99.91	Hot	3.09	99.44	Hot
22:00	3.21	99.7	Hot	2.96	98.92	Warm
23:00	2.97	98.92	Warm	2.77	97.48	Warm
0:00	2.74	97.14	Warm	2.56	94.66	Warm

Table 5. PMV, PPD, and thermal sensation for the west room in the U-shaped building in the baseline case and with optimum shading devices 1.25 m long

Time (h)	PMV U-shaped Baseline	PPD U-shaped Baseline (%)	Sensation U-shaped Baseline	PMV U-shaped Combined	PPD U-shaped Combined (%)	Sensation U-shaped Combined
1:00	2.43	91.82	Warm	2.15	83.08	Warm
2:00	2.22	85.6	Warm	1.96	75.09	Slightly warm
3:00	2.01	77.31	Warm	1.78	66.01	Slightly warm
4:00	1.84	69.31	Slightly warm	1.63	58.41	Slightly warm
5:00	1.7	61.89	Slightly warm	1.51	51.57	Slightly warm
6:00	1.71	62.32	Slightly warm	1.5	51.03	Slightly warm
7:00	2	76.63	Warm	1.64	59.03	Slightly warm
8:00	2.44	91.93	Warm	1.81	67.91	Slightly warm
9:00	2.71	96.89	Warm	1.83	68.83	Slightly warm
10:00	2.86	98.32	Warm	1.91	72.81	Slightly warm
11:00	2.9	98.63	Warm	2.06	79.59	Warm
12:00	2.87	98.4	Warm	2.22	85.77	Warm
13:00	2.88	98.45	Warm	2.3	88.28	Warm
14:00	3.01	99.15	Hot	2.38	90.58	Warm
15:00	3.21	99.71	Hot	2.46	92.68	Warm
16:00	3.42	99.92	Hot	2.58	94.97	Warm
17:00	3.5	99.96	Hot	2.71	96.94	Warm
18:00	3.46	99.94	Hot	2.77	97.54	Warm
19:00	3.34	99.87	Hot	2.77	97.55	Warm
20:00	3.21	99.72	Hot	2.72	97.08	Warm
21:00	3.07	99.38	Hot	2.65	96.1	Warm
22:00	2.87	98.35	Warm	2.52	93.82	Warm
23:00	2.65	95.97	Warm	2.32	88.85	Warm
0:00	2.41	91.27	Warm	2.09	80.86	Warm

human body in W/m^2 , P_a is the partial pressure of water vapor in Pa, determined as follows:

$$P_a = 10 - 5\Phi \exp \left[\frac{-5800}{t_a} + 0.048T_a + 4.1 \times 10^{-8} t_a^3 + 6.545 \ln T_a \right], \quad (2)$$

t_a is the air temperature in $^{\circ}C$, Φ is the relative humidity, $T_a = t_a + 273.15$ in K, t_r is the mean radiation temperature in $^{\circ}C$, determined as follows:

$$t_r = t_g + 2.4v_a 0.5(t_g - t_a) \quad (3)$$

v_a is the average air speed in m/s, t_g is the temperature of the black sphere, f_{cl} is the clothing area factor, determined as follows:

$$f_{cl} = 1.0 + 0.3I_{cl} \quad (4)$$

t_{cl} is the clothing area temperature in $^{\circ}C$, determined as follows:

$$t_{cl} = 35.7 - 0.028(M - W) - I_{cl} \times \left\{ \begin{array}{l} 3.96 \times 10^{-8} f_{cl} \times \\ \times \left[(t_{cl} + 273)^4 - (t_r + 273)^4 - (f_{cl} - t_a) \right] \end{array} \right\} \quad (5)$$

and h_c is the surface heat transfer coefficient in $W/(m^2 \cdot K)$, determined as follows:

$$h_c = \begin{cases} 2.38(t_{cl} - t_a)^{0.25}, & \text{if } 2.38(t_{cl} - t_a)^{0.25} \geq 12.1\sqrt{v_a} \\ 12.1\sqrt{v_a}, & \text{if } 2.38(t_{cl} - t_a)^{0.25} < 12.1\sqrt{v_a} \end{cases} \quad (6)$$

The PPD and PMV indicators have the following relationship (Duan et al., 2022; Rînjea et al., 2022):

$$PPD = 100 - 95e^{\left[(-0.335.PMV^4 - 0.217.PMV^2) \right]} \quad (7)$$

In this work, the PMV and PPD values were obtained by setting the environmental variables extracted from the EnergyPlus simulation program (air temperature, relative humidity, air speed, and mean radiant temperature) as well as the personal variables (thermal resistance of clothing and metabolic rate) in the OpenStudio platform. The thermal resistance of clothing was considered to be equal to 0.5, which represents light summer clothing, and the metabolic rate was taken as 1.25 met (1 met = 58 W/m^2) to represent the routine and relaxed state.

The hourly variation of the PMV and PPD values, corresponding to different building forms on July 21, was determined for the baseline case without shading and for the case with the combined shading device 1.25 m long (Tables 3–5). The results show that with the shading device, most of daily hours are brought closer to the comfort zone. In the rectangular building, the sensation percentages for hot, warm, and slightly warm for the baseline case were 29.16%, 62.5%, and 8.33%, respectively. With the combined shading, they became 0% for hot sensation, 66.67% for warm sensation, and 33.33% for slightly warm sensation, indicating significant shifting closer to the

comfort zone. In addition, combined shading in the L-shaped building brings daily hours' percentage for indoor sensation from 33.33% in the baseline case to 16.67% in the case with combined shading for hot sensation, 58.33% in the baseline case to 66.67% in the case with combined shading for warm sensation, and 8.33% in the baseline case to 16.67% in the case with combined shading for slightly warm sensation, indicating good shifting for sensation to the comfort zone. Combined shading in the U-shaped building brings daily hours' percentage for indoor sensation from 33.33% for hot sensation, 54.17% for warm sensation, and 12.5% for slightly warm sensation for the baseline conditions to 0%, 62.5%, and 37.5%, respectively, indicating significant shifting for sensation closer to the comfort zone.

Based on these results, it can be concluded that combined shading of an optimal length of 1.25 m obviously improves the sensation feeling in all buildings. The rectangular and U-shaped buildings show better results than the L-shaped building. This can be attributed to the compactness factor of the rectangular building, which has less surface to volume ratio for the building envelope exposed to the direct sunlight, while the U-shaped building is characterized by self-shading since its shape creates more shadows.

Besides, Tables 3–5 it also show that the PPD percentage for all buildings significantly decreases with the presence of shading devices for all day long as compared with the case without shading, which indicates obvious improvement of the thermal comfort in the rooms with shading.

Conclusions

This papers addresses the impact of different shading devices of different length on the thermal performance and thermal comfort of different residential building forms in hot-dry climate in Amman, Jordan. Based on the results, we can draw the following conclusions:

- Vertical fins facing west make almost no difference in all types of buildings except for the rectangular one, which shows maximum reduction in the indoor air temperature of 0.6 $^{\circ}C$.
- Horizontal and combined shadings demonstrate significant reduction in the indoor air temperature and enhance the thermal performance.
- The length of shading is a significant factor in improving the indoor temperature, and it was found that 1.25 m length ensures the best performance, minimizing the air temperature in all building forms.
- Combined shading shows the best results as compared with other types of shading as it reduces the indoor air temperature by 2.6–3.3 $^{\circ}C$ for all building forms.
- Combined shading with 1.25 m in length can improve the thermal comfort of all buildings, especially in rectangular and U-shaped buildings,

where hot sensation was minimized. This is explained by the compactness and self-shading factors.

- The U-shaped building shows the best PMV and PPD results when using combined shading with 1.25 m in length since 0%, 62.5%, and 37.5%

for hot, warm, and slightly warm sensation were recorded, respectively. The rectangular building shows the largest air temperature reduction when using combined shading with 1.25 m in length as it reduces the air temperature by 3.3°C at 4:00 PM.

References

- Abdulla, F. (2020). 21st century climate change projections of precipitation and temperature in Jordan. *Procedia Manufacturing*, Vol. 44, pp. 197–204. DOI: 10.1016/j.promfg.2020.02.222.
- Abu Qadourah, J., Al-Falahat, A. M., Alwashdeh, S. S., and Nytsch-Geusen, C. (2022). Improving the energy performance of the typical multi-family buildings in Amman, Jordan. *City, Territory and Architecture*, Vol. 9, 6. DOI: 10.1186/s40410-022-00151-8.
- Albatayneh, A., Jaradat, M., Al-Omary, M., and Zaquot, M. (2021). Evaluation of coupling PV and air conditioning vs. solar cooling systems—case study from Jordan. *Applied Science*, Vol. 11, Issue 2, 511. DOI: 10.3390/app11020511.
- Ali, H. and Hashlamun, R. (2019). Envelope retrofitting strategies for public school buildings in Jordan. *Journal of Building Engineering*, Vol. 25, 100819. DOI: 10.1016/j.jobbe.2019.100819.
- Bataineh, K. and Alrabee, A. (2018). Improving the energy efficiency of the residential buildings in Jordan. *Buildings*, Vol. 8, Issue 7, 85. DOI: 10.3390/buildings8070085.
- Bataineh, K. and Al Rabee, A. (2021). Design optimization of energy efficient residential buildings in Mediterranean region. *Journal of Sustainable Development of Energy, Water and Environment Systems*, Vol. 10, Issue 2, 1090385. DOI: 10.13044/j.sdewes.d9.0385.
- Duan, X., Yu, S., Chu, J., Chen, D., and Chen, Y. (2022). Evaluation of indoor thermal environments using a novel predicted mean vote model based on artificial neural networks. *Buildings*, Vol. 12, Issue 11, 1880. DOI: 10.3390/buildings12111880.
- Emir, S. (2016). The evaluation of thermal comfort on primary schools in hot-humid climates: a case study for Antalya. *European Journal of Sustainable Development*, Vol. 5, No. 1, 53. DOI: 10.14207/ejsd.2016.v5n1p53.
- Eskandari, H., Saedvandi, M., and Mahdavinjad, M. (2018). The impact of Iwan as a traditional shading device on the building energy consumption. *Buildings*, Vol. 8, Issue 1, 3. DOI: 10.3390/buildings8010003.
- Fanger, P. O. (1970). Thermal comfort. Copenhagen: Danish Technical Press, 244 p.
- Fanger, P. O and Toftum, J. (2002). Extension of the PMV model to non-air-conditioned buildings in warm climates. *Energy and Building*, Vol. 34, Issue 6, pp. 533–536. DOI: 10.1016/S0378-7788(02)00003-8.
- Feng, F., Kunwar, N., Cetin, K., and O'Neill, Z. (2021). A critical review of fenestration/window system design methods for high performance buildings. *Energy and Buildings*, Vol. 248, 111184. DOI: 10.1016/j.enbuild.2021.111184.
- Freewan, A. A. Y. (2014). Impact of external shading devices on thermal and daylighting performance of offices in hot climate regions. *Solar Energy*, Vol. 102, pp. 14–30. DOI: 10.1016/j.solener.2014.01.009.
- GIASMA (2022). Sunrise, sunset, dawn and dusk times around the world. [online] Available at: <https://www.gaisma.com/en> [Date accessed September, 2022].
- Hailu, H., Gelan, E., and Girma, Y. (2021). Indoor thermal comfort analysis: a case study of modern and traditional buildings in hot-arid climatic region of Ethiopia. *Urban Science*, Vol. 5, Issue 3, 53. DOI: 10.3390/urbansci5030053.
- Kumar, P. and Sharma, A. (2022). Assessing outdoor thermal comfort conditions at an urban park during summer in the hot semi-arid region of India. *Materials Today: Proceedings*, Vol. 61, Part 2, pp. 356–369. DOI: 10.1016/j.matpr.2021.10.085.
- Minangi, F. S. and Alibaba, H. Z. (2018). Effect of shading on thermal performance of dormitory building on hot climate. *International Journal of Interdisciplinary Research and Innovation*, Vol. 6, Issue 4, pp. 610–621.
- Mushtaha, E., Salameh, T., Kharrufa, S., Mori, T., Aldawoud, A., Hamad, R., and Nemer, T. (2021). The impact of passive design strategies on cooling loads of buildings in temperate climate. *Case Studies in Thermal Engineering*, Vol. 28, 101588. DOI: 10.1016/j.csite.2021.101588.
- Nwankwo, P. N., Akpado, K. A., Isizoh, A. N., Alumona, T. L., and Oguejiofor, O. S. (2021). Optimization of solar panel tilt and azimuth angle for maximum solar irradiation and minimum loss for rural electrification. *International Journal for Research in Applied Science & Engineering Technology (IJRASET)*, Vol. 9, Issue X, pp. 1852–1868. DOI: 10.22214/ijraset.2021.38665.
- Ohene, E., Shu-Chien, H., and Chan, A. P. C. (2022). Feasibility and retrofit guidelines towards net-zero energy buildings in tropical climates: a case of Ghana. *Energy and Buildings*, Vol. 269, 112252. DOI: 10.1016/j.enbuild.2022.112252.
- Rinjea, C., Chivu, O. R., Darabont, D.-C., Feier, A. I., Borda, C., Gheorghe, M., and Nitoi, D. F. (2022). Influence of the thermal environment on occupational health and safety in automotive industry: a case study. *International Journal of Environmental Research and Public Health*, Vol. 19, Issue 14, 8572. DOI: 10.3390/ijerph19148572.